

Polariton interactions in microcavities with atomically thin semiconductor layers

O. Bleu, J. Levinsen, and M. M. Parish

*School of Physics and Astronomy, Monash University, Victoria 3800, Australia and
ARC Centre of Excellence in Future Low-Energy Electronics Technologies, Monash University, Victoria 3800, Australia*

We investigate the interactions between exciton-polaritons in N two-dimensional semiconductor layers embedded in a planar microcavity. In the limit of low-energy and low-momentum scattering, where we can ignore the composite nature of the excitons, we obtain exact analytical expressions for the spin-triplet and spin-singlet interaction strengths, which go beyond the Born approximation employed in previous calculations. Crucially, we find that the strong light-matter coupling enhances the strength of polariton-polariton interactions compared to that of the exciton-exciton interactions, with the latter vanishing in the zero-momentum limit. We furthermore show that the polariton interactions have a highly non-trivial dependence on the number of layers N , and we highlight the important role played by the optically dark states that exist in multiple layers. In particular, we predict that the singlet interaction strength is stronger than the triplet one for a wide range of parameters in most of the currently used transition metal dichalcogenides. This has consequences for the pursuit of polariton condensation and other interaction-driven phenomena in these materials.

Microcavity exciton-polaritons (polaritons) are quasi-particles that arise from the strong coupling between semiconductor excitons (bound electron-hole pairs) and cavity photon resonances. Due to their excitonic component, polaritons interact with each other, in contrast to bare photons in vacuum. This interaction is the cornerstone of a variety of observed phenomena ranging from optical parametric scattering [1] and bistability [2], to Bose-Einstein condensation [3, 4], superfluidity [5] and the formation of quantized vortices [6]. Hence, semiconductor microcavities are fruitful platforms to investigate two-dimensional (2D) quantum fluids of light [7–10].

Atomically thin semiconductors in the form of transition metal dichalcogenides (TMDs) have recently emerged as promising materials for realizing polaritonic phenomena at room temperature, due to the large exciton binding energies in TMD monolayers [11–14]. Furthermore, TMDs can be made nearly disorder free, unlike organic materials [15], and they can be externally tuned using electrostatic gating [14], which is an essential tool for any future optoelectronic devices [16]. Already, a strong exciton-photon (Rabi) coupling has been observed in both TMD monolayer [17–20] and multilayer structures [21, 22]. In particular, the use of multilayer van der Waals heterostructures can generate large Rabi couplings [23] as well as provide routes towards engineering other material properties [24]. However, it is an open and non-trivial question how the polariton-polariton interactions depend on experimental parameters such as the light polarization [25] and the number of layers in these systems. The answer to this question impacts the highly active investigation of interaction-induced nonlinear optical properties [26–30] and the ongoing quest [31] to realize polariton condensation in pure TMD systems.

In this Letter, we address this question by studying the effective interactions between polaritons in a system of N identical 2D layers embedded in a planar microcavity. A key simplification of our work is to assume

that the energy scale of polariton-polariton scattering is smaller than the exciton binding energy, thus allowing us to neglect the composite nature of the excitons and treat them as structureless bosons with contact interactions and mass m_X . This is a reasonable assumption in the case of TMD layers, where the exciton binding energy is much larger than all other relevant energy scales [14, 23]. Solving the scattering problem of two lower polaritons at zero momentum, we obtain the following *exact* expression for the polariton-polariton interaction strength:

$$T_{\sigma\sigma'} = \frac{4\pi\hbar^2 X_0^4}{m_X N \ln\left(\frac{E_{\sigma\sigma'}}{2|E_0^L|}\right)} \equiv \begin{cases} \alpha_1, & \sigma = \sigma' \\ \alpha_2, & \sigma \neq \sigma'. \end{cases} \quad (1)$$

Here $E_{\sigma\sigma'} > 0$ are the energies associated with the spin-triplet ($\sigma = \sigma'$) and spin-singlet ($\sigma \neq \sigma'$) exciton scattering lengths, where $\sigma = \pm$ encodes the pseudo-spin (circular polarization) of the exciton (photon). X_0^2 and E_0^L are, respectively, the exciton fraction and the energy (relative to the exciton energy) of the zero-momentum lower polariton, which depend on the number of layers N via the exciton-photon Rabi coupling. Crucially, Eq. (1) differs from the usual case of 2D quantum particles with short-range interactions, where the scattering *vanishes* in the zero-momentum limit [32, 33]. Hence the strong light-matter coupling *enhances* the polariton-polariton interaction strength with respect to the corresponding exciton-exciton interaction strength. Equation (1) is a key result of this work, which we derive in the following.

Dark, bright and polariton states.— We start with the single-polariton Hamiltonian that describes the coupling between the cavity photon and N monolayer excitonic modes:

$$\hat{H}_0 = \sum_{\mathbf{k},\sigma} E_{\mathbf{k}}^C \hat{c}_{\mathbf{k}\sigma}^\dagger \hat{c}_{\mathbf{k}\sigma} + \sum_{\mathbf{k},\sigma} \sum_{n=1}^N E_{\mathbf{k}}^X \hat{x}_{\mathbf{k}\sigma,n}^\dagger \hat{x}_{\mathbf{k}\sigma,n} + \frac{\hbar g_R}{2} \sum_{\mathbf{k},\sigma} \sum_{n=1}^N \left(\hat{x}_{\mathbf{k}\sigma,n}^\dagger \hat{c}_{\mathbf{k}\sigma} + \hat{c}_{\mathbf{k}\sigma}^\dagger \hat{x}_{\mathbf{k}\sigma,n} \right), \quad (2)$$

where $\hat{c}_{\mathbf{k}\sigma}$ ($\hat{c}_{\mathbf{k}\sigma}^\dagger$) and $\hat{x}_{\mathbf{k}\sigma,n}$ ($\hat{x}_{\mathbf{k}\sigma,n}^\dagger$) are bosonic annihilation (creation) operators of cavity photons and monolayer excitons, respectively, with in-plane momentum $\hbar\mathbf{k}$ and layer index n . The kinetic energies at low momenta are $E_{\mathbf{k}}^C = \hbar^2 k^2 / 2m_C + \delta$ and $E_{\mathbf{k}}^X = \hbar^2 k^2 / 2m_X$, where $k \equiv |\mathbf{k}|$ and we measure energies with respect to the exciton energy at zero momentum. Thus, δ is the photon-exciton detuning, while m_C and m_X are the photon and exciton masses, respectively. Here, for simplicity, we consider identical monolayers that are located at the maxima of the electric field within the cavity, so that both $E_{\mathbf{k}}^X$ and the exciton-photon coupling g_R are independent of n . However, it is straightforward to generalize our results to the case of a layer-dependent light-matter coupling. We furthermore assume that g_R is independent of polarization/spin and we neglect any splittings between the longitudinal and transverse modes of the excitons [34–36] and photons [37]. Hence, there is no spin-orbit coupling [38–41] in our model, but such a single-particle effect should not strongly affect the short-distance two-body scattering processes considered here.

The spin-degenerate eigenstates of Eq. (2) consist of two polariton modes (upper and lower branches) and $N-1$ dark states which are decoupled from light [42, 43]. The multilayer system is frequently described by a two-coupled-mode exciton-photon model with a renormalized Rabi coupling [9], but here, we keep track of the complete structure of the eigenstates. Since only the bright states [in-phase superpositions of all monolayer excitons, as depicted in Fig. 1(a)] couple to light, one can rewrite the Hamiltonian in the corresponding convenient basis:

$$\hat{H}_0 = \sum_{\mathbf{k},\sigma} \left[E_{\mathbf{k}}^C \hat{c}_{\mathbf{k}\sigma}^\dagger \hat{c}_{\mathbf{k}\sigma} + E_{\mathbf{k}}^X \left(\hat{b}_{\mathbf{k}\sigma}^\dagger \hat{b}_{\mathbf{k}\sigma} + \sum_{l=1}^{N-1} \hat{d}_{\mathbf{k}\sigma,l}^\dagger \hat{d}_{\mathbf{k}\sigma,l} \right) \right] + \frac{\hbar\Omega_R}{2} \sum_{\mathbf{k},\sigma} \left(\hat{b}_{\mathbf{k}\sigma}^\dagger \hat{c}_{\mathbf{k}\sigma} + \hat{c}_{\mathbf{k}\sigma}^\dagger \hat{b}_{\mathbf{k}\sigma} \right), \quad (3)$$

where $\hat{b}_{\mathbf{k}\sigma}$ and $\hat{d}_{\mathbf{k}\sigma,l}$ are the annihilation operators for bright and dark excitonic states, respectively, which are related to the bare monolayer exciton operators via the unitary transformation:

$$\hat{d}_{\mathbf{k}\sigma,l} = \sum_{n=1}^N u_{ln} \hat{x}_{\mathbf{k}\sigma,n}, \quad \hat{b}_{\mathbf{k}\sigma} \equiv \hat{d}_{\mathbf{k}\sigma,N} = \sum_{n=1}^N \frac{\hat{x}_{\mathbf{k}\sigma,n}}{\sqrt{N}} \quad (4)$$

with $u_{ln} = \frac{1}{\sqrt{N}} e^{i2\pi nl/N}$ [44]. The multilayer nature of the bright states gives rise to an enhanced Rabi coupling $\hbar\Omega_R = \hbar g_R \sqrt{N}$, thus making it easier to access the strong-coupling regime in a multilayer structure. The diagonal form of the exciton-photon Hamiltonian is then:

$$\hat{H}_0 = \sum_{\mathbf{k},\sigma} \left[E_{\mathbf{k}}^L \hat{L}_{\mathbf{k}\sigma}^\dagger \hat{L}_{\mathbf{k}\sigma} + E_{\mathbf{k}}^U \hat{U}_{\mathbf{k}\sigma}^\dagger \hat{U}_{\mathbf{k}\sigma} + \sum_{l=1}^{N-1} E_{\mathbf{k}}^X \hat{d}_{\mathbf{k}\sigma,l}^\dagger \hat{d}_{\mathbf{k}\sigma,l} \right],$$

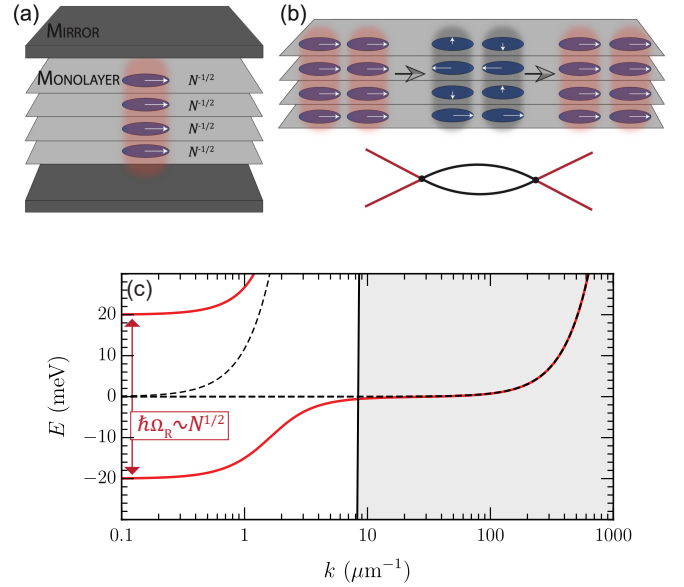


Figure 1. (a) Schematic illustration of the microcavity structure with N embedded monolayers, where $N = 4$. A polariton consists of a cavity photon (shaded red) and a superposition of N in-phase 2D excitons (blue ellipses), where the relative phase of each exciton is represented by an in-plane arrow. (b) Example of a scattering process involving intermediate dark states which are uncoupled to light. (c) Polariton dispersion (red) at zero detuning, together with the uncoupled cavity photon and excitonic modes (dashed black lines). For high momenta $k > \epsilon_X/\hbar c$ (shaded region), where ϵ_X is the exciton energy and c is the speed of light, the exciton is far detuned in energy from the photon and thus essentially uncoupled. We use the parameters for MoSe₂ (see Table I) with $\epsilon_X = 1.66\text{eV}$ [21] and $N = 4$ layers.

with \hat{L} (\hat{U}) the lower (upper) polariton annihilation operators defined in the standard way

$$\begin{pmatrix} \hat{L}_{\mathbf{k}\sigma} \\ \hat{U}_{\mathbf{k}\sigma} \end{pmatrix} = \begin{pmatrix} X_{\mathbf{k}} & C_{\mathbf{k}} \\ -C_{\mathbf{k}} & X_{\mathbf{k}} \end{pmatrix} \begin{pmatrix} \hat{b}_{\mathbf{k}\sigma} \\ \hat{c}_{\mathbf{k}\sigma} \end{pmatrix}. \quad (5)$$

Here $E_{\mathbf{k}}^{U,L}$ are the polariton eigen-energies [see Fig. 1(c)],

$$E_{\mathbf{k}}^{U,L} = \frac{1}{2} \left(E_{\mathbf{k}}^X + E_{\mathbf{k}}^C \pm \sqrt{(E_{\mathbf{k}}^C - E_{\mathbf{k}}^X)^2 + \hbar^2 \Omega_R^2} \right), \quad (6)$$

and $X_{\mathbf{k}}, C_{\mathbf{k}}$ are the Hopfield coefficients, corresponding to exciton and photon fractions:

$$X_{\mathbf{k}}^2 = \frac{1}{2} \left(1 + \frac{E_{\mathbf{k}}^C - E_{\mathbf{k}}^X}{E_{\mathbf{k}}^U - E_{\mathbf{k}}^L} \right), \quad C_{\mathbf{k}}^2 = 1 - X_{\mathbf{k}}^2. \quad (7)$$

Exciton-exciton interactions.— Since the layer spacing is typically larger than the exciton size, we may assume that the interactions between excitons only occur within the same layer. Furthermore, if the scattering energy is small compared to the exciton binding energy (as is the case in TMDs [14]), then we can describe the ex-

citon interactions with an *s*-wave contact potential [45],

$$\hat{V} = \sum_{n=1}^N \sum_{\substack{\mathbf{k}, \mathbf{k}', \mathbf{q} \\ \sigma, \sigma'}} \frac{g_{\sigma\sigma'}}{2} \hat{x}_{\mathbf{k}+\mathbf{q}\sigma, n}^\dagger \hat{x}_{\mathbf{k}'-\mathbf{q}\sigma', n}^\dagger \hat{x}_{\mathbf{k}'\sigma', n} \hat{x}_{\mathbf{k}\sigma, n}, \quad (8)$$

where the “bare” spin-dependent coupling strength $g_{\sigma\sigma'}$ is independent of layer index n since we have assumed that the monolayers are identical. Also, we have set the monolayer area to 1. We emphasize that our approach is different from determining the exciton-exciton interaction strength within the Born approximation, as in previous works [46–52]. This approximation effectively estimates $g_{\sigma\sigma'}$ from the microscopic structure of the excitons, whereas here we solve the low-energy scattering problem exactly and treat $g_{\sigma\sigma'}$ as a bare parameter that must be related to experimental observables [53]. As such, we impose a cutoff Λ on the relative scattering momentum, which we will send to infinity at the end of the calculation (for details, see the Supplemental Material [54]).

Transforming to the bright-dark-exciton basis using Eq. (4), the interaction term becomes:

$$\hat{V} = \sum_{\{l_j\}} \delta_{\mathcal{M}} \sum_{\substack{\mathbf{k}, \mathbf{k}', \mathbf{q} \\ \sigma, \sigma'}} \frac{g_{\sigma\sigma'}}{2N} \hat{d}_{\mathbf{k}+\mathbf{q}\sigma, l_1}^\dagger \hat{d}_{\mathbf{k}'-\mathbf{q}\sigma', l_2}^\dagger \hat{d}_{\mathbf{k}'\sigma', l_3} \hat{d}_{\mathbf{k}\sigma, l_4}, \quad (9)$$

where $\{l_j\} = \{l_1, l_2, l_3, l_4\}$. The kronecker delta ($\delta_{\mathcal{M}} = 1$ if $\mathcal{M} = 0$, $\delta_{\mathcal{M}} = 0$ otherwise) encodes the phase selection rule for binary scatterings illustrated in Fig. 1(b), where $\mathcal{M} = \text{Mod}[l_1 + l_2 - l_3 - l_4, N]$. It is worth noting that the interaction coupling constant is reduced by the factor of $1/N$ in the new bright-dark-states basis. Moreover, written in this form, Eq. (9) can involve a huge number of terms (N^3 for each spin channel). This highlights the complexity of the scattering processes which can occur in any multilayer structure in the strong-coupling regime.

Two-polariton scattering.— To investigate polariton-polariton interactions, we consider the two-body scattering problem at zero center-of-mass momentum. The two-particle states are $|A_\sigma, B_{\sigma'}, \mathbf{k}\rangle = \hat{A}_{-\mathbf{k}\sigma}^\dagger \hat{B}_{\mathbf{k}\sigma'}^\dagger |0\rangle$, where the operators \hat{A} , \hat{B} can correspond to lower polaritons \hat{L} , upper polaritons \hat{U} or dark-exciton operators \hat{d}_l , with $l = 1, 2, \dots, N-1$. To proceed, we employ the *T*-matrix operator, which is given by the Born series

$$\hat{T}(E) = \hat{V} + \hat{V} \frac{1}{E - \hat{H}_0 + i0} \hat{V} + \dots \quad (10)$$

where E is the scattering energy and $+i0$ represents an infinitesimal positive imaginary part. The interaction strength for lower polaritons is then given by the matrix element

$$T_{\sigma\sigma'}(k) \equiv \frac{\langle L_\sigma, L_{\sigma'}, \mathbf{k}' | \hat{T}(2E_{\mathbf{k}}^L) | L_\sigma, L_{\sigma'}, \mathbf{k} \rangle}{1 + \delta_{\sigma\sigma'}}, \quad (11)$$

with the on-shell condition $|\mathbf{k}'| = |\mathbf{k}| = k$. Here the normalization factor in the denominator accounts for scattering between identical particles. The Born approximation to the interaction strength corresponds to keeping only the first term in the series, which gives $g_{\sigma\sigma'} X_{\mathbf{k}}^4 / N$. However, higher order terms will significantly modify this result since they can involve scattering into dark intermediate states, as illustrated in Fig. 1(b).

Remarkably, we find that the low-energy polariton *T* matrix takes the simple form [54]

$$T_{\sigma\sigma'}(k) = \frac{X_{\mathbf{k}}^4}{\frac{N}{g_{\sigma\sigma'}} - \Pi(2E_{\mathbf{k}}^L)}. \quad (12)$$

Here, the one-loop polarization bubble $\Pi(E)$ is extremely well approximated by that of N exciton pairs:

$$\Pi(E) \simeq N \sum_{\mathbf{q}}^{\Lambda} \frac{1}{E - 2E_{\mathbf{q}}^X + i0}, \quad (13)$$

since the exciton scattering is dominated by large momenta where the photon is far off resonant [see Fig. 1(c)]. This is a consequence of the photon mass being orders of magnitude smaller than the exciton mass, $m_C \ll m_X$.

To obtain cutoff-independent results, we relate the bare couplings to physical observables as follows [33]

$$\frac{1}{g_{\sigma\sigma'}} = - \sum_{\mathbf{q}}^{\Lambda} \frac{1}{E_{\sigma\sigma'} + 2E_{\mathbf{q}}^X}, \quad (14)$$

where we have introduced the physical energy scales $E_{\sigma\sigma'} = \frac{\hbar^2}{2m_r a_{\sigma\sigma'}^2}$ related to the 2D exciton *s*-wave scattering lengths $a_{\sigma\sigma'}$ and the two-exciton reduced mass $m_r = m_X/2$. Note that the scattering parameters are intrinsic to the monolayer and are independent of N . In the singlet case, $E_{+-} = E_{-+} = E_B^{XX}$ corresponds to the binding energy of the biexciton (bound state of two excitons). Due to Pauli exclusion, there is no triplet biexciton state, but the triplet scattering length is well defined and is of the order of the 2D exciton Bohr radius $a_{\sigma\sigma} \sim a_B$ [54]; hence we have $E_{\sigma\sigma} \sim 2E_B^X$.

Inserting Eq. (14) into Eq. (12) and taking the limit $\Lambda \rightarrow \infty$, one obtains the cutoff-independent *T* matrix

$$T_{\sigma\sigma'}(k) = \frac{4\pi\hbar^2 X_{\mathbf{k}}^4}{m_X N \ln\left(\frac{E_{\sigma\sigma'}}{2|E_{\mathbf{k}}^L|}\right)}. \quad (15)$$

The limit $k \rightarrow 0$ finally yields $T_{\sigma\sigma'}$ in Eq. (1), which gives the lower polariton effective interaction “constants” for the triplet (α_1) and singlet (α_2) channels at zero momentum (a similar procedure can be used to evaluate the scattering between upper polaritons). In the absence of light-matter coupling, we recover the usual 2D two-body *T* matrix for quantum particles in a monolayer [32], $\frac{4\pi\hbar^2}{m_X} \left[\ln\left(\frac{E_{\sigma\sigma'}}{2E_{\mathbf{k}}^X}\right) + i\pi \right]^{-1}$, which we see vanishes in the

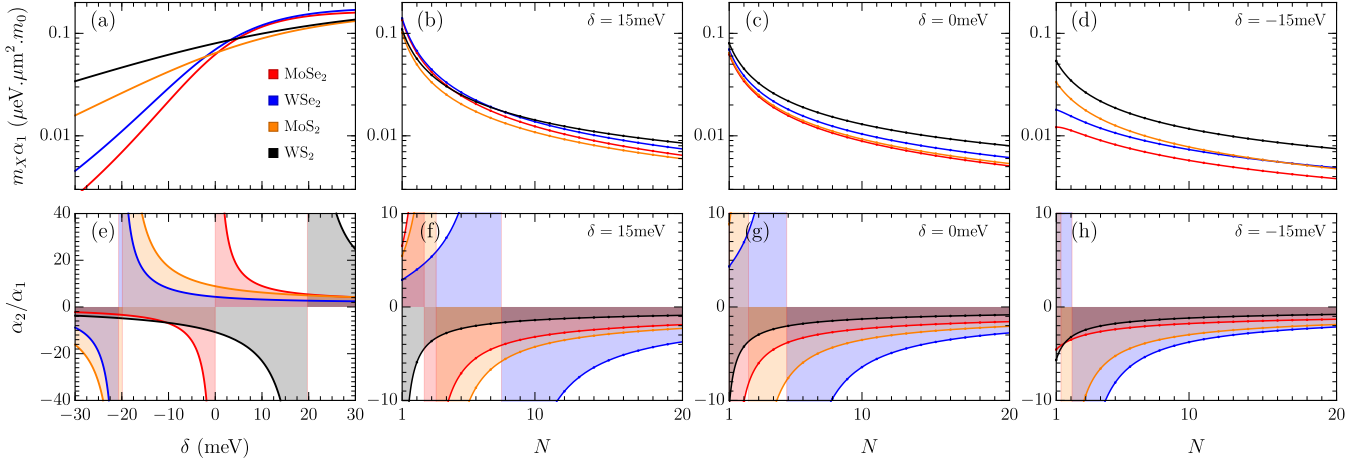


Figure 2. Polariton interactions in several 2D materials. (a,e) Monolayer triplet interactions α_1 and the corresponding singlet-triplet ratio α_2/α_1 as a function of the exciton-photon detuning δ . (b-d) Multilayer triplet interactions as a function of N for different δ , and (f-g) the corresponding singlet-triplet ratio. Parameters are taken from Table I, with m_0 the free electron mass.

limit of zero momentum. Within Bogoliubov theory [55], this implies that the ground-state energy of a dilute gas of 2D excitons will feature a *logarithmic* dependence on density, in contrast to what has been observed for polariton condensates [52].

Implications for experiment.— Equations (1) and (15) show that the lower polariton interaction strength is enhanced compared to the monolayer exciton interaction strength because the strong light-matter coupling shifts the scattering energy in the low-momentum limit. In particular, Eq. (1) explains why the polariton blueshift in experiment scales linearly with condensate density [52], unlike for the case of standard 2D bosons [55]. Note that Eq. (1) is a low-energy expression that is valid in the regime $|E_0^L| \ll E_B^X$. Thus, we expect our predictions for α_1 and α_2 to be accurate in the case of TMD layers due to their sizeable exciton binding energies, where $E_B^X \gtrsim 10\hbar g_R$ (see Table I).

Figures 2(a-d) show the polariton triplet interaction strength α_1 for a range of photon-exciton detunings δ in different 2D TMD systems. Similar to previous predictions within the Born approximation, α_1 is repulsive and increases with increasing δ (corresponding to an increasing exciton fraction X_0^2). However, we see that a larger number of layers N typically *suppresses* the polariton interaction strength by a factor of $\sim N$ plus logarithmic corrections. This suggests that the strongest polariton interactions occur in monolayer TMDs, while the largest Rabi coupling is achieved with multiple layers. For the case of monolayer MoSe₂, the value of α_1 at detuning $\delta \simeq -15\text{ meV}$ is consistent with the recent low-density measurements reported in Refs. [28, 29], thus confirming the validity of our model.

In contrast to the triplet case, the polariton singlet interaction strength α_2 can display a scattering resonance

Table I. Experimental values used in Fig. 2 for the monolayer Rabi splitting ($\hbar g_R$), exciton (E_B^X) and biexciton (E_B^{XX}) binding energies, all in units of meV.

Material	MoSe ₂	WSe ₂	MoS ₂	WS ₂
$\hbar g_R$	20 [21]	23.5 [19]	46 [17]	70 [18]
E_B^X	470 [21]	370 [11, 59]	960 [17]	700 [18]
E_B^{XX}	20 [60]	52 [59]	70 [61]	53 [62]

when $2|E_0^L| \approx E_{+-}$, corresponding to the point where the lower polariton branch crosses the biexciton energy. Such resonances are present in Figs. 2(e-h), where we have plotted the singlet/triplet ratio (α_2/α_1) for each TMD system. Here we see that the sign and magnitude of α_2 can be tuned by varying δ and/or N . Furthermore, these panels demonstrate that the singlet interaction is in general stronger than the triplet one for a wide range of experimental parameters. To our knowledge, this important feature has not been noticed previously. In particular, a large and negative α_2/α_1 can destabilize a polariton condensate, which possibly explains why condensation has been challenging to achieve thus far. Furthermore, the sizeable and tunable α_2 in TMDs opens up the possibility of realizing strongly correlated phenomena such as polariton blockade [56], bipolariton superfluidity [57] and polaron physics [58].

The singlet resonance effectively corresponds to the polariton “Feshbach resonance” [63] experimentally investigated in single GaAs quantum wells [64, 65]. Note that GaAs-based microcavities are qualitatively different from the TMD case since they typically have $|\alpha_2|/\alpha_1 < 1$ [66], except in a narrow parameter region close to the biexciton resonance [63], and moreover the exciton binding energy is not necessarily the largest energy scale — for example, for the case of 12 quantum wells, we have

$\hbar\Omega_R \gtrsim E_B^X$ [52]. On the other hand, neither TMDs nor GaAs quantum wells are expected to feature a triplet polariton Feshbach resonance. While Eq. (1) naively predicts a resonance at $|E_0^L| \simeq E_B^X$, such a large energy scale goes beyond the validity of our model and requires a more precise description of the short-distance physics such as the composite nature of the excitons and the layer thickness. A full microscopic description of polariton interactions is beyond the scope of the present work.

Finally, we emphasize that most of the intermediate states appearing in the T matrix are dark states [Fig. 1(b)] which lie at the exciton energy. In the present work, these are virtual states which only contribute to the final strength of polariton interactions. However, in principle they can be turned into real long-lived excitons via additional scattering processes, for example mediated by phonons [67, 68], and they can therefore populate an excitonic reservoir.

Conclusions.— We have derived exact analytical expressions for the polariton-polariton triplet and singlet interaction strengths in TMD layers embedded in a planar microcavity. Crucially, we have demonstrated that the strong exciton-photon coupling enhances the polariton interactions relative to those of bare excitons. Furthermore, we have analyzed the dependence on the number of layers and we have exposed the important role of optically dark states in multilayer polariton-polariton scattering. Our results suggest that the singlet interaction is stronger than the triplet one for a range of TMD heterostructures, which has important consequences for realizing polariton condensation and other interaction-driven phenomena in these systems. In particular, a large repulsive singlet interaction can lead to the formation of spin-polarized domains, and thus to spin-resolved ultralow threshold lasing.

We are grateful to G. Li, F. M. Marchetti, E. Ostrovskaya, and M. Pieczarka for useful discussions. We acknowledge support from the Australian Research Council Centre of Excellence in Future Low-Energy Electronics Technologies (CE170100039). JL is also supported through the Australian Research Council Future Fellowship FT160100244.

-
- densation of exciton polaritons*, *Nature* **443**, 409 (2006).
- [4] R. Balili, V. Hartwell, D. Snoke, L. Pfeiffer, and K. West, *Bose-Einstein Condensation of Microcavity Polaritons in a Trap*, *Science* **316**, 1007 (2007).
 - [5] A. Amo, J. Lefrre, S. Pigeon, C. Adrados, C. Ciuti, I. Carusotto, R. Houdr, E. Giacobino, and A. Bramati, *Superfluidity of polaritons in semiconductor microcavities*, *Nature Physics* **5**, 805 (2009).
 - [6] K. G. Lagoudakis, M. Wouters, M. Richard, A. Baas, I. Carusotto, R. Andr, L. S. Dang, and B. Deveaud-Plédran, *Quantized vortices in an exciton-polariton condensate*, *Nature Physics* **4**, 706 (2008).
 - [7] J. Keeling, F. M. Marchetti, M. H. Szymaska, and P. B. Littlewood, *Collective coherence in planar semiconductor microcavities*, *Semiconductor Science and Technology* **22**, R1 (2007).
 - [8] H. Deng, H. Haug, and Y. Yamamoto, *Exciton-polariton Bose-Einstein condensation*, *Rev. Mod. Phys.* **82**, 1489 (2010).
 - [9] I. Carusotto and C. Ciuti, *Quantum fluids of light*, *Rev. Mod. Phys.* **85**, 299 (2013).
 - [10] A. Kavokin, J. J. Baumberg, G. Malpuech, and F. P. Laussy, *Microcavities* (Oxford university press, 2017).
 - [11] K. He, N. Kumar, L. Zhao, Z. Wang, K. F. Mak, H. Zhao, and J. Shan, *Tightly Bound Excitons in Monolayer WSe₂*, *Phys. Rev. Lett.* **113**, 026803 (2014).
 - [12] Z. Ye, T. Cao, K. O'Brien, H. Zhu, X. Yin, Y. Wang, S. G. Louie, and X. Zhang, *Probing excitonic dark states in single-layer tungsten disulphide*, *Nature* **513**, 214 (2014).
 - [13] A. Chernikov, T. C. Berkelbach, H. M. Hill, A. Rigosi, Y. Li, O. B. Aslan, D. R. Reichman, M. S. Hybertsen, and T. F. Heinz, *Exciton Binding Energy and Nonhydrogenic Rydberg Series in Monolayer WS₂*, *Phys. Rev. Lett.* **113**, 076802 (2014).
 - [14] G. Wang, A. Chernikov, M. M. Glazov, T. F. Heinz, X. Marie, T. Amand, and B. Urbaszek, *Colloquium: Excitons in atomically thin transition metal dichalcogenides*, *Rev. Mod. Phys.* **90**, 021001 (2018).
 - [15] O. V. Mikhnenko, P. W. M. Blom, and T.-Q. Nguyen, *Exciton diffusion in organic semiconductors*, *Energy Environ. Sci.* **8**, 1867 (2015).
 - [16] D. Sanvitto and S. Kna-Cohen, *The road towards polaritonic devices*, *Nature Materials* **15**, 1061 (2016).
 - [17] X. Liu, T. Galfsky, Z. Sun, F. Xia, E.-c. Lin, Y.-H. Lee, S. Kna-Cohen, and V. M. Menon, *Strong lightmatter coupling in two-dimensional atomic crystals*, *Nature Photonics* **9**, 3034 (2014).
 - [18] L. C. Flatten, Z. He, D. M. Coles, A. A. P. Trichet, A. W. Powell, R. A. Taylor, J. H. Warner, and J. M. Smith, *Room-temperature exciton-polaritons with two-dimensional WS₂*, *Scientific Reports* **6**, 33134 (2016).
 - [19] N. Lundt, S. Klembt, E. Cherotchenko, S. Betzold, O. Iff, A. V. Nalitov, M. Klaas, C. P. Dietrich, A. V. Kavokin, S. Hfling, and C. Schneider, *Room-temperature Tamm-plasmon exciton-polaritons with a WSe₂ monolayer*, *Nature Communications* **7**, 13328 (2016).
 - [20] M. Sidler, P. Back, O. Cotlet, A. Srivastava, T. Fink, M. Kroner, E. Demler, and A. Imamoglu, *Fermi polaron-polaritons in charge-tunable atomically thin semiconductors*, *Nature Physics* **13**, 255 (2017).
 - [21] S. Dufferwiel, S. Schwarz, F. Withers, A. A. P. Trichet, F. Li, M. Sich, O. Del Pozo-Zamudio, C. Clark, A. Nalitov, D. D. Solnyshkov, G. Malpuech, K. S. Novoselov, J. M. Smith, M. S. Skolnick, D. N. Krizhanovskii, and

-
- [1] P. G. Savvidis, J. J. Baumberg, R. M. Stevenson, M. S. Skolnick, D. M. Whittaker, and J. S. Roberts, *Angle-Resonant Stimulated Polariton Amplifier*, *Phys. Rev. Lett.* **84**, 1547 (2000).
 - [2] A. Baas, J. P. Karr, H. Eleuch, and E. Giacobino, *Optical bistability in semiconductor microcavities*, *Phys. Rev. A* **69**, 023809 (2004).
 - [3] J. Kasprzak, M. Richard, S. Kundermann, A. Baas, P. Jeambrun, J. M. J. Keeling, F. M. Marchetti, M. H. Szymaska, R. Andr, J. L. Staehli, V. Savona, P. B. Littlewood, B. Deveaud, and L. S. Dang, *Bose-Einstein con-*

- A. I. Tartakovskii, *Exciton-polaritons in van der Waals heterostructures embedded in tunable microcavities*, *Nature Communications* **6**, 8579 (2015).
- [22] M. Krl, K. Rechciska, K. Nogajewski, M. Grzeszczyk, K. empicka, R. Mirek, S. Piotrowska, K. Watanabe, T. Taniguchi, M. R. Molas, M. Potemski, J. Szczytko, and B. Pitka, *Exciton-polaritons in multilayer WSe₂ in a planar microcavity*, *2D Materials* **7**, 015006 (2019).
- [23] C. Schneider, M. M. Glazov, T. Korn, S. Hfling, and B. Urbaszek, *Two-dimensional semiconductors in the regime of strong light-matter coupling*, *Nature Communications* **9**, 2695 (2018).
- [24] A. K. Geim and I. V. Grigorieva, *Van der Waals heterostructures*, *Nature* **499**, 419 (2013).
- [25] I. A. Shelykh, A. V. Kavokin, Y. G. Rubo, T. C. H. Liew, and G. Malpuech, *Polariton polarization-sensitive phenomena in planar semiconductor microcavities*, *Semiconductor Science and Technology* **25**, 013001 (2009).
- [26] G. Scuri, Y. Zhou, A. A. High, D. S. Wild, C. Shu, K. De Greve, L. A. Jauregui, T. Taniguchi, K. Watanabe, P. Kim, M. D. Lukin, and H. Park, *Large Excitonic Reflectivity of Monolayer MoSe₂ Encapsulated in Hexagonal Boron Nitride*, *Phys. Rev. Lett.* **120**, 037402 (2018).
- [27] F. Barachati, A. Fieramosca, S. Hafezian, J. Gu, B. Chakraborty, D. Ballarini, L. Martinu, V. Menon, D. Sanvitto, and S. Kna-Cohen, *Interacting polariton fluids in a monolayer of tungsten disulfide*, *Nature Nanotechnology* **13**, 906 (2018).
- [28] L. B. Tan, O. Cotlet, A. Bergschneider, R. Schmidt, P. Back, Y. Shimazaki, M. Kroner, and A. Imamoglu, *Interacting Polaron-Polaritons* (2019), arXiv:1903.05640 [cond-mat.mes-hall].
- [29] R. P. A. Emmanuel, M. Sich, O. Kyriienko, V. Shahnazaryan, F. Withers, A. Catanzaro, P. M. Walker, F. A. Benimetskiy, M. S. Skolnick, A. I. Tartakovskii, I. A. Shelykh, and D. N. Krizhanovskii, *Highly nonlinear trion-polaritons in a monolayer semiconductor* (2019), arXiv:1910.14636 [cond-mat.mes-hall].
- [30] J. Gu, V. Walther, L. Waldecker, D. Rhodes, A. Raja, J. C. Hone, T. F. Heinz, S. Kena-Cohen, T. Pohl, and V. M. Menon, *Enhanced nonlinear interaction of polaritons via excitonic Rydberg states in monolayer WSe₂* (2019), arXiv:1912.12544 [cond-mat.mtrl-sci].
- [31] M. Waldherr, N. Lundt, M. Klaas, S. Betzold, M. Wurdack, V. Baumann, E. Estrecho, A. Nalitov, E. Cherotchenko, H. Cai, E. A. Ostrovskaya, A. V. Kavokin, S. Tongay, S. Klembt, S. Hfling, and C. Schneider, *Observation of bosonic condensation in a hybrid monolayer MoSe₂-GaAs microcavity*, *Nature Communications* **9**, 3286 (2018).
- [32] S. K. Adhikari, *Quantum scattering in two dimensions*, *American Journal of Physics* **54**, 362 (1986).
- [33] J. Levinsen and M. M. Parish, *Strongly interacting two-dimensional Fermi gases*, *Annu. Rev. Cold Atoms Mol. Phys.* **3**, 1 (2015).
- [34] M. Z. Maialle, E. A. de Andrade e Silva, and L. J. Sham, *Exciton spin dynamics in quantum wells*, *Phys. Rev. B* **47**, 15776 (1993).
- [35] M. M. Glazov, T. Amand, X. Marie, D. Lagarde, L. Bouet, and B. Urbaszek, *Exciton fine structure and spin decoherence in monolayers of transition metal dichalcogenides*, *Phys. Rev. B* **89**, 201302 (2014).
- [36] T. Yu and M. W. Wu, *Valley depolarization due to inter-valley and intravalley electron-hole exchange interactions in monolayer MoS₂*, *Phys. Rev. B* **89**, 205303 (2014).
- [37] G. Panzarini, L. C. Andreani, A. Armitage, D. Baxter, M. S. Skolnick, V. N. Astratov, J. S. Roberts, A. V. Kavokin, M. R. Vladimirova, and M. A. Kaliteevski, *Exciton-light coupling in single and coupled semiconductor microcavities: Polariton dispersion and polarization splitting*, *Phys. Rev. B* **59**, 5082 (1999).
- [38] A. Kavokin, G. Malpuech, and M. Glazov, *Optical Spin Hall Effect*, *Phys. Rev. Lett.* **95**, 136601 (2005).
- [39] C. Leyder, M. Romanelli, J. P. Karr, E. Giacobino, T. C. H. Liew, M. M. Glazov, A. V. Kavokin, G. Malpuech, and A. Bramati, *Observation of the optical spin Hall effect*, *Nature Physics* **3**, 628 (2007).
- [40] O. Bleu, D. D. Solnyshkov, and G. Malpuech, *Optical valley Hall effect based on transitional metal dichalcogenide cavity polaritons*, *Phys. Rev. B* **96**, 165432 (2017).
- [41] N. Lundt, L. Dusanowski, E. Sedov, P. Stepanov, M. M. Glazov, S. Klembt, M. Klaas, J. Beierlein, Y. Qin, S. Tongay, M. Richard, A. V. Kavokin, S. Höfling, and C. Schneider, *Optical valley Hall effect for highly valley-coherent exciton-polaritons in an atomically thin semiconductor*, *Nature Nanotechnology* **14**, 770775 (2019).
- [42] E. Ivchenko, A. Nesvizhskii, and S. Jorda, *Resonant Bragg reflection from quantum-well structures*, *Superlattices and Microstructures* **16**, 17 (1994).
- [43] A. Kavokin and G. Malpuech, *Cavity polaritons*, Vol. 32 (Elsevier, 2003).
- [44] A similar transformation has been considered in Ref. [69], but its explicit mathematical form was not given.
- [45] L. D. Landau and E. M. Lifshitz, *Quantum mechanics: non-relativistic theory*, Vol. 3 (Elsevier, 2013).
- [46] C. Ciuti, V. Savona, C. Piermarocchi, A. Quattropani, and P. Schwendimann, *Role of the exchange of carriers in elastic exciton-exciton scattering in quantum wells*, *Phys. Rev. B* **58**, 7926 (1998).
- [47] F. Tassone and Y. Yamamoto, *Exciton-exciton scattering dynamics in a semiconductor microcavity and stimulated scattering into polaritons*, *Phys. Rev. B* **59**, 10830 (1999).
- [48] G. Rochat, C. Ciuti, V. Savona, C. Piermarocchi, A. Quattropani, and P. Schwendimann, *Excitonic Bloch equations for a two-dimensional system of interacting excitons*, *Phys. Rev. B* **61**, 13856 (2000).
- [49] M. Combescot, O. Betbeder-Matibet, and F. Dubin, *The many-body physics of composite bosons*, *Physics Reports* **463**, 215 (2008).
- [50] M. M. Glazov, H. Ouerdane, L. Pilozzi, G. Malpuech, A. V. Kavokin, and A. D'Andrea, *Polariton-polariton scattering in microcavities: A microscopic theory*, *Phys. Rev. B* **80**, 155306 (2009).
- [51] V. Shahnazaryan, I. Iorsh, I. A. Shelykh, and O. Kyriienko, *Exciton-exciton interaction in transition-metal dichalcogenide monolayers*, *Phys. Rev. B* **96**, 115409 (2017).
- [52] E. Estrecho, T. Gao, N. Bobrovska, D. Comber-Todd, M. D. Fraser, M. Steger, K. West, L. N. Pfeiffer, J. Levinsen, M. M. Parish, T. C. H. Liew, M. Matuszewski, D. W. Snoke, A. G. Truscott, and E. A. Ostrovskaya, *Direct measurement of polariton-polariton interaction strength in the Thomas-Fermi regime of exciton-polariton condensation*, *Phys. Rev. B* **100**, 035306 (2019).
- [53] C. Mora and Y. Castin, *Ground State Energy of the Two-Dimensional Weakly Interacting Bose Gas: First Correction Beyond Bogoliubov Theory*, *Phys. Rev. Lett.* **102**, 180404 (2009).

- [54] See supplemental material for details on how we calculate the polariton-polariton T matrix, and a discussion of low-energy triplet exciton-exciton scattering in two dimensions.
- [55] V. N. Popov, *On the theory of the superfluidity of two- and one-dimensional bose systems*, *Theoretical and Mathematical Physics* **11**, 565 (1972).
- [56] I. Carusotto, T. Volz, and A. Imamoglu, *Feshbach blockade: Single-photon nonlinear optics using resonantly enhanced cavity polariton scattering from biexciton states*, *EPL (Europhysics Letters)* **90**, 37001 (2010).
- [57] F. M. Marchetti and J. Keeling, *Collective Pairing of Resonantly Coupled Microcavity Polaritons*, *Phys. Rev. Lett.* **113**, 216405 (2014).
- [58] J. Levinsen, F. M. Marchetti, J. Keeling, and M. M. Parish, *Spectroscopic Signatures of Quantum Many-Body Correlations in Polariton Microcavities*, *Phys. Rev. Lett.* **123**, 266401 (2019).
- [59] Y. You, X.-X. Zhang, T. C. Berkelbach, M. S. Hybertsen, D. R. Reichman, and T. F. Heinz, *Observation of biexcitons in monolayer WSe₂*, *Nature Physics* **11**, 477 (2015).
- [60] K. Hao, J. F. Specht, P. Nagler, L. Xu, K. Tran, A. Singh, C. K. Dass, C. Schller, T. Korn, M. Richter, and et al., *Neutral and charged inter-valley biexcitons in monolayer MoSe₂*, *Nature Communications* **8**, 15552 (2017).
- [61] C. Mai, A. Barrette, Y. Yu, Y. G. Semenov, K. W. Kim, L. Cao, and K. Gundogdu, *Many-Body Effects in Valleytronics: Direct Measurement of Valley Lifetimes in Single-Layer MoS₂*, *Nano Lett.* **14**, 202 (2014).
- [62] P. Nagler, M. V. Ballottin, A. A. Mitioglu, M. V. Durnev, T. Taniguchi, K. Watanabe, A. Chernikov, C. Schüller, M. M. Glazov, P. C. M. Christianen, and T. Korn, *Zeeman Splitting and Inverted Polarization of Biexciton Emission in Monolayer WS₂*, *Phys. Rev. Lett.* **121**, 057402 (2018).
- [63] M. Wouters, *Resonant polariton-polariton scattering in semiconductor microcavities*, *Phys. Rev. B* **76**, 045319 (2007).
- [64] N. Takemura, S. Trebaol, M. Wouters, M. T. Portella-Oberli, and B. Deveaud, *Polaritonic Feshbach resonance*, *Nature Physics* **10**, 500 (2014).
- [65] N. Takemura, M. D. Anderson, M. Navadeh-Toupchi, D. Y. Oberli, M. T. Portella-Oberli, and B. Deveaud, *Spin anisotropic interactions of lower polaritons in the vicinity of polaritonic Feshbach resonance*, *Phys. Rev. B* **95**, 205303 (2017).
- [66] M. Vladimirova, S. Cronenberger, D. Scalbert, K. V. Kavokin, A. Miard, A. Lemaître, J. Bloch, D. Solnyshkov, G. Malpuech, and A. V. Kavokin, *Polariton-polariton interaction constants in microcavities*, *Phys. Rev. B* **82**, 075301 (2010).
- [67] C. Piermarocchi, F. Tassone, V. Savona, A. Quattropani, and P. Schwendimann, *Nonequilibrium dynamics of free quantum-well excitons in time-resolved photoluminescence*, *Phys. Rev. B* **53**, 15834 (1996).
- [68] I. G. Savenko, T. C. H. Liew, and I. A. Shelykh, *Stochastic Gross-Pitaevskii Equation for the Dynamical Thermalization of Bose-Einstein Condensates*, *Phys. Rev. Lett.* **110**, 127402 (2013).
- [69] G. C. L. Rocca, F. Bassani, and V. M. Agranovich, *Biexcitons and dark states in semiconductor microcavities*, *J. Opt. Soc. Am. B* **15**, 652 (1998).
- [70] R. Takayama, N. H. Kwong, I. Rumyantsev, M. Kuwata-Gonokami, and R. Binder, *T-matrix analysis of biexcitonic correlations in the nonlinear optical response of semiconductor quantum wells*, *The European Physical Journal B - Condensed Matter and Complex Systems* **25**, 445 (2002).

SUPPLEMENTAL MATERIAL: “POLARITON INTERACTIONS IN MICROCAVITIES WITH ATOMICALLY THIN SEMICONDUCTOR LAYERS”

O. Bleu, J. Levinsen, M. M. Parish

*School of Physics and Astronomy, Monash University, Victoria 3800, Australia and
ARC Centre of Excellence in Future Low-Energy Electronics Technologies, Monash University, Victoria 3800, Australia*

T-MATRIX

Here, we provide some details for the T -matrix calculation for the scattering between two lower polaritons. First, we recall the bosonic commutation rules:

$$[\hat{A}_{\mathbf{k}\sigma}, \hat{B}_{\mathbf{k}'\sigma'}^\dagger] = \delta_{AB} \delta_{\sigma\sigma'} \delta_{\mathbf{k}\mathbf{k}'}, \quad (\text{S1})$$

where \hat{A} , \hat{B} can correspond to lower polaritons \hat{L} , upper polaritons \hat{U} or dark-exciton operators \hat{d}_l , with $l = 1, 2, \dots, N - 1$. The two-particle states with zero total momentum are defined as:

$$|A_\sigma, B_{\sigma'}, \mathbf{k}\rangle = \hat{A}_{-\mathbf{k}\sigma}^\dagger \hat{B}_{\mathbf{k}\sigma'}^\dagger |0\rangle, \quad (\text{S2})$$

with the scalar product:

$$\langle A_{\sigma_1}, B_{\sigma'_1}, \mathbf{k}_1 | C_{\sigma_2}, D_{\sigma'_2}, \mathbf{k}_2 \rangle = \langle 0 | \hat{B}_{\mathbf{k}_1\sigma'_1} \hat{A}_{-\mathbf{k}_1\sigma_1} \hat{C}_{-\mathbf{k}_2\sigma_2}^\dagger \hat{D}_{\mathbf{k}_2\sigma'_2}^\dagger | 0 \rangle \quad (\text{S3})$$

$$= \delta_{BC} \delta_{AD} \delta_{\sigma'_1\sigma_2} \delta_{\sigma_1\sigma'_2} \delta_{\mathbf{k}_1, -\mathbf{k}_2} + \delta_{BD} \delta_{AC} \delta_{\sigma_1\sigma_2} \delta_{\sigma'_1\sigma'_2} \delta_{\mathbf{k}_1\mathbf{k}_2}. \quad (\text{S4})$$

The non-interacting eigenvalues are given by

$$\hat{H}_0 |A_\sigma, B_{\sigma'}, \mathbf{k}\rangle = \sum_J \sum_{\mathbf{q}, s} E_{\mathbf{q}}^J \hat{J}_{\mathbf{q}s}^\dagger \hat{J}_{\mathbf{q}s} \hat{A}_{-\mathbf{k}\sigma}^\dagger \hat{B}_{\mathbf{k}\sigma'}^\dagger |0\rangle \quad (\text{S5})$$

$$= (E_{-\mathbf{k}}^A + E_{\mathbf{k}}^B) \hat{A}_{-\mathbf{k}\sigma}^\dagger \hat{B}_{\mathbf{k}\sigma'}^\dagger |0\rangle \quad (\text{S6})$$

$$= (E_{-\mathbf{k}}^A + E_{\mathbf{k}}^B) |A_\sigma, B_{\sigma'}, \mathbf{k}\rangle, \quad (\text{S7})$$

where the sum on J in the first line accounts for all the available single-particle energy states, and $E_{\mathbf{q}}^J \equiv E_{\mathbf{q}}^X$ for all the dark states with $\hat{J} = \hat{d}_l$.

Now we consider the scattering between two lower polaritons, the first term of the Born series gives:

$$\langle L_\sigma, L_{\sigma'}, \mathbf{k}' | \hat{V} | L_\sigma, L_{\sigma'}, \mathbf{k} \rangle = X_{\mathbf{k}'}^2 X_{\mathbf{k}}^2 \frac{g_{\sigma\sigma'}}{N} (1 + \delta_{\sigma\sigma'}). \quad (\text{S8})$$

(Notice that $g_{+-} = g_{-+}$, and $g_{++} = g_{--}$). Higher order terms in the T -matrix involve dark or upper polariton intermediate states. It is useful to introduce the matrix element between two lower polaritons and an arbitrary two-particle state

$$\langle A_\sigma, B_{\sigma'}, \mathbf{k}' | \hat{V} | L_\sigma, L_{\sigma'}, \mathbf{k} \rangle = \frac{g_{\sigma\sigma'} X_{\mathbf{k}}^2}{N} (1 + \delta_{\sigma\sigma'}) \begin{cases} \delta_{\text{Mod}[l_1+l_2, N]}, & A = d_{l_1}, B = d_{l_2}, l_1, l_2 \neq N \\ X_{\mathbf{k}'}^2, & A = L, B = L \\ C_{\mathbf{k}'}^2, & A = U, B = U \\ -X_{\mathbf{k}'} C_{\mathbf{k}'}, & A = L, B = U \\ -X_{\mathbf{k}'} C_{\mathbf{k}'}, & A = U, B = L, \end{cases} \quad (\text{S9})$$

and the completeness relation

$$\mathbb{1} = \frac{1}{2} \sum_{\mathbf{q}} \sum_{A,B} \sum_{s,s'} |A_s, B_{s'}, \mathbf{q}\rangle \langle A_s, B_{s'}, \mathbf{q}|, \quad (\text{S10})$$

which satisfies the usual property of the identity

$$\mathbb{1}|C_\sigma, D_{\sigma'}, \mathbf{k}\rangle = \frac{1}{2} \sum_{\mathbf{q}} \sum_{A,B} \sum_{s,s'} |A_s, B_{s'}, \mathbf{q}\rangle \langle A_s, B_{s'}, \mathbf{q}| C_\sigma, D_{\sigma'}, \mathbf{k}\rangle \quad (\text{S11})$$

$$= \frac{1}{2} \sum_{\mathbf{q}} (|C_\sigma, D_{\sigma'}, \mathbf{q}\rangle \delta_{\mathbf{q}\mathbf{k}} + |D_{\sigma'}, C_\sigma, \mathbf{q}\rangle \delta_{\mathbf{q},-\mathbf{k}}) \quad (\text{S12})$$

$$= \frac{1}{2} (|C_\sigma, D_{\sigma'}, \mathbf{k}\rangle + |D_{\sigma'}, C_\sigma, -\mathbf{k}\rangle) \quad (\text{S13})$$

$$= |C_\sigma, D_{\sigma'}, \mathbf{k}\rangle. \quad (\text{S14})$$

Then the second-order term reads

$$\langle L^\sigma, L^{\sigma'}, \mathbf{k}' | \hat{V} \frac{1}{E - \hat{H}_0} \hat{V} | L^\sigma, L^{\sigma'}, \mathbf{k}\rangle = \langle L^\sigma, L^{\sigma'}, \mathbf{k}' | \hat{V} \mathbb{1} \frac{1}{E - \hat{H}_0} \hat{V} | L^\sigma, L^{\sigma'}, \mathbf{k}\rangle \quad (\text{S15})$$

$$= (1 + \delta_{\sigma\sigma'}) \left(\frac{g_{\sigma\sigma'}}{N} \right)^2 X_{\mathbf{k}}^2 X_{\mathbf{k}'}^2 \quad (\text{S16})$$

$$\times \sum_{\mathbf{q}} \left[\frac{X_{\mathbf{q}}^4}{E - 2E_{\mathbf{q}}^L} + \frac{C_{\mathbf{q}}^4}{E - 2E_{\mathbf{q}}^U} + \frac{2C_{\mathbf{q}}^2 X_{\mathbf{q}}^2}{E - E_{\mathbf{q}}^L - E_{\mathbf{q}}^U} + \sum_{l_1, l_2}^{N-1} \frac{\delta_{\text{Mod}[l_1+l_2, N]}}{E - 2E_{\mathbf{q}}^X} \right]$$

$$= (1 + \delta_{\sigma\sigma'}) \frac{g_{\sigma\sigma'} X_{\mathbf{k}}^4}{N} \frac{g_{\sigma\sigma'}}{N} \Pi(E), \quad (\text{S17})$$

where we have used $|\mathbf{k}'| = |\mathbf{k}|$ in the last line. The one-loop polarization bubble, $\Pi(E)$, is given by

$$\Pi(E) = \underbrace{\sum_{\mathbf{q}}^{\Lambda} \frac{X_{\mathbf{q}}^4}{E - 2E_{\mathbf{q}}^L} + \sum_{\mathbf{q}}^{\Lambda} \frac{C_{\mathbf{q}}^4}{E - 2E_{\mathbf{q}}^U}}_{\Pi_P(E)} + 2 \underbrace{\sum_{\mathbf{q}}^{\Lambda} \frac{X_{\mathbf{q}}^2 C_{\mathbf{q}}^2}{E - E_{\mathbf{q}}^L - E_{\mathbf{q}}^U}}_{\Pi_X(E)} + (N-1) \underbrace{\sum_{\mathbf{q}}^{\Lambda} \frac{1}{E - 2E_{\mathbf{q}}^X}}_{\Pi_X(E)}, \quad (\text{S18})$$

where we have introduced the high-energy cutoff wavevector Λ .

The generalisation to higher order terms leads to

$$\langle L_\sigma, L_{\sigma'}, \mathbf{k}' | \hat{T}(E) | L_\sigma, L_{\sigma'}, \mathbf{k}\rangle = (1 + \delta_{\sigma\sigma'}) \frac{g_{\sigma\sigma'} X_{\mathbf{k}}^4}{N} \left[1 + \frac{g_{\sigma\sigma'}}{N} \Pi(E) + \left(\frac{g_{\sigma\sigma'}}{N} \Pi(E) \right)^2 + \dots \right] \quad (\text{S19})$$

$$= (1 + \delta_{\sigma\sigma'}) \frac{X_{\mathbf{k}}^4}{\left(\frac{N}{g_{\sigma\sigma'}} - \Pi(E) \right)}, \quad (\text{S20})$$

which after rearranging the prefactor, gives the formula (12) presented in the main text. Note that $\Pi(E)$ also contains a factor N . The integrals in $\Pi(E)$ are dominated by the large wavevectors \mathbf{q} , where $E_{\mathbf{q}}^L \rightarrow E_{\mathbf{q}}^X$, $X_{\mathbf{q}}^2 \rightarrow 1$, $C_{\mathbf{q}}^2 \rightarrow 0$ and one can neglect the second and third terms. Thus, $\Pi(E)$ simply reduces to $N \times \Pi_X(E)$. This approximation is valid because $m_C \ll m_X$ as explained below.

$m_C \ll m_X$ and $\Pi(E)$ approximation

The approximation of the one-loop polarization bubble [Eq. (S18)] relies on the very large ratio between the cavity photon and the exciton masses ($m_C/m_X \sim 10^{-4} - 10^{-5}$). This approximation is equivalent to neglecting the low- \mathbf{q} behavior of the integrand in:

$$\Pi_P(E) = \frac{1}{2\pi} \int_0^{\Lambda} q dq \left(\frac{X_{\mathbf{q}}^4}{E - 2E_{\mathbf{q}}^L} + \frac{C_{\mathbf{q}}^4}{E - 2E_{\mathbf{q}}^U} + 2 \frac{X_{\mathbf{q}}^2 C_{\mathbf{q}}^2}{E - E_{\mathbf{q}}^L - E_{\mathbf{q}}^U} \right). \quad (\text{S21})$$

To analytically evaluate if this low- \mathbf{q} behavior plays a role, one can approximate the integrand in two domains with the following replacements:

- $q < q_0$: $E_{\mathbf{q}}^L \rightarrow \tilde{E}_{\mathbf{q}}^L = \hbar^2 q^2 / 2m_L + E_0^L$, $E_{\mathbf{q}}^U \rightarrow \tilde{E}_{\mathbf{q}}^U = \hbar^2 q^2 / 2m_U + E_0^U$, $C_{\mathbf{q}} \rightarrow C_0$, $X_{\mathbf{q}} \rightarrow X_0$
- $q > q_0$: $E_{\mathbf{q}}^L \rightarrow E_{\mathbf{q}}^X$, $C_{\mathbf{q}} \rightarrow 0$, $X_{\mathbf{q}} \rightarrow 1$.

The inflection wavevector q_0 and the lower (upper) polariton effective masses m_L , (m_U) are defined as:

$$q_0 = \frac{\sqrt{2m_p|E_0^L|}}{\hbar}, \quad m_L = \frac{m_C}{C_0^2}, \quad m_U = \frac{m_C}{X_0^2}. \quad (\text{S22})$$

This gives

$$\Pi_P(E) \simeq \frac{1}{2\pi} \int_0^{q_0} q dq \left(\frac{X_0^4}{E - 2\tilde{E}_{\mathbf{q}}^L} + \frac{C_0^4}{E - 2\tilde{E}_{\mathbf{q}}^U} + 2 \frac{X_0^2 C_0^2}{E - \tilde{E}_{\mathbf{q}}^L - \tilde{E}_{\mathbf{q}}^U} \right) + \frac{1}{2\pi} \int_{q_0}^{\Lambda} q dq \left(\frac{1}{E - 2E_{\mathbf{q}}^X} \right) \quad (\text{S23})$$

$$= \frac{m_C}{4\pi\hbar^2 C_0^2 X_0^2} \left[X_0^6 \ln \left(\frac{2E_0^L - E}{-E} \right) + C_0^6 \ln \left(\frac{2E_0^U - E}{2E_0^U - E + 2|E_0^L|X_0^2/C_0^2} \right) + 4X_0^4 C_0^4 \ln \left(\frac{(\delta - E)C_0^2 X_0^2}{C_0^2(\delta - E) + |E_0^L|} \right) \right] \\ + \frac{m_X}{4\pi\hbar^2} \ln \left(\frac{E - 2|E_0^L|C_0^2 m_C/m_X}{E - 2E_{\Lambda}^X} \right) \quad (\text{S24})$$

$$\simeq \frac{m_X}{4\pi\hbar^2} \ln \left(\frac{E}{E - 2E_{\Lambda}^X} \right) = \sum_{\mathbf{q}}^{\Lambda} \frac{1}{E - 2E_{\mathbf{q}}^X}. \quad (\text{S25})$$

Hence, one can see that in the limit $m_C/m_X \rightarrow 0$, $\Pi_P(E) \rightarrow \Pi_X(E)$, and Eq. (S18) reduces to $\Pi(E) \simeq N\Pi_X(E)$.

TRIPLET EXCITON-EXCITON SCATTERING

In the main text, we assume that the exciton triplet scattering length is of the order of the exciton Bohr radius a_B . Here, we motivate this assumption by recalling that this is the case for 2D hard disk particles of radius r_0 . For low-energy particles, the two-body scattering is dominated by the s wave contribution, and the center of mass wavefunction obeys the 2D radial Schrödinger equation [45]

$$-\frac{\hbar^2}{2m_r} \frac{1}{r} \frac{\partial}{\partial r} \left(r \frac{\partial \psi}{\partial r} \right) + U(r)\psi = E\psi, \quad (\text{S26})$$

with m_r the two-body reduced mass. The hard disk potential corresponds to an infinitely high potential barrier of radius r_0

$$U = \begin{cases} \infty, & r \leq r_0 \\ 0, & r > r_0. \end{cases} \quad (\text{S27})$$

Outside the potential, the general solution is a superposition of first and second kind Bessel functions

$$\psi(r) = AJ_0(kr) + BY_0(kr), \quad (\text{S28})$$

with $k = \sqrt{2m_r E}/\hbar$. Then, using its asymptotic form, one introduces the scattering phase shift δ_s

$$\psi(r) \xrightarrow[r \rightarrow \infty]{} \sqrt{\frac{2}{\pi kr}} (A \cos(kr - \pi/4) + B \sin(kr - \pi/4)) = \sqrt{\frac{2}{\pi kr}} C \cos(kr - \pi/4 + \delta_s), \quad (\text{S29})$$

with

$$\tan(\delta_s) = -\frac{B}{A}. \quad (\text{S30})$$

The continuity of the wavefunction at $r = r_0$ gives the relation:

$$\cot(\delta_s) = -\frac{A}{B} = \frac{Y_0(kr_0)}{J_0(kr_0)}. \quad (\text{S31})$$

Finally, taking the low-energy (low- k) limit one obtains

$$\cot(\delta_s) = \frac{2}{\pi} \ln(ka_s), \quad (\text{S32})$$

where we have introduced the 2D scattering length a_s

$$a_s = \frac{e^\gamma r_0}{2} \simeq 0.89r_0, \quad (\text{S33})$$

with $\gamma = 0.577\dots$ the Euler-Mascheroni constant.

The corresponding hard disc triplet exciton T -matrix reads:

$$T_{\sigma\sigma}(k) = \frac{2\pi\hbar^2}{m_r} \left[\ln\left(\frac{E_{\sigma\sigma}}{E}\right) + i\pi \right]^{-1}, \quad (\text{S34})$$

with

$$E_{\sigma\sigma} = \frac{\hbar^2}{2m_r a_s^2}. \quad (\text{S35})$$

Note that a similar form for the low-energy T matrix has been obtained in Ref. [70] which accounts for the composite (electron-hole) nature of the exciton in the limit of equal electron and hole masses.